Information Dynamics and Applications
https://www.acadlore.com/journals/IDA

An Optimized Algorithm for Peak to Average Power Ratio Reduction in Orthogonal Frequency Division Multiplexing Communication Systems: An Integrated Approach

Rathod Shivaji[1], Nataraj Kanathur Ramaswamy[1], Mallikarjunaswamy Srikantaswamy[2*], Rekha Kanathur Ramaswamy[3]

[1] Department of Electronics and Communication Engineering, Don Bosco Institute of Technology, 560074 Bengaluru, India
[2] Department of Electronics and Communication Engineering, JSS Academy of Technical Education, 560060 Bengaluru, India
[3] Department of Electronics and Communication Engineering, SJB Institute of Technology, 560060 Bengaluru, India

[*] Correspondence: Mallikarjunaswamy Srikantaswamy (fund.impfile@gmail.com)

Received: 05-11-2023 **Revised:** 06-18-2023 **Accepted:** 07-10-2023

Citation: R. Shivaji, N. K. Ramaswamy, M. Srikantaswamy, and R. K. Ramaswamy, "An optimized algorithm for peak to average power ratio reduction in orthogonal frequency division multiplexing communication systems: An integrated approach," *Inf. Dyn. Appl.*, vol. 2, no. 3, pp. 115–125, 2023. https://doi.org/10.56578/ida020301.

Abstract: The impact of the Peak to Average Power Ratio (PAPR) on the efficiency of an Orthogonal Frequency Division Multiplexing (OFDM) communication system is significantly mitigated through an innovative Reconfigurable Integrated Algorithm (RIA). In this study, the RIA combines the advantages of Partial Transmit Sequence (PTS) and Companding Transformation (CT) techniques, enhancing the overall efficiency while reducing the signal distortion inherent in linear transformation methods. A unique reconfiguration process enables integration of PTS and CT to minimize PAPR. This process considers key parameters including multi-channel inputs and delay attenuation factors. Comparison of the RIA with conventional methods such as PTS, CT, selective mapping (SLM), and Tone Reservation (TR) reveals superior performance, as evidenced by the Complementary Cumulative Distribution Function (CCDFs) curve. Implementations of the algorithm using MATLAB R2022a demonstrate significant improvements in PAPR performance, showing gains of 0.55dB and 0.656dB compared to the PTS and CT methods respectively. Moreover, the novel RIA methodology exhibits enhanced transmission rates and lower Bit Error Rates (BER) relative to conventional methods. In conclusion, the proposed RIA offers a promising approach for optimizing OFDM system performance through efficient PAPR reduction. Its implementation can drive the advancement of telecommunications technologies and further understanding of OFDM communication systems.

Keywords: Average Power Ratio; Orthogonal Frequency Division Multiplexing; Bit Error Rates; Complementary Cumulative Distribution Function; Companding Transformation

1 Introduction

OFDM has emerged as a widely adopted method for multicarrier modulation, acclaimed for enhancing spectrum efficiency while concurrently improving immunity to inter-symbol interference (ISI) and multipath interference [1–3]. However, the nature of OFDM signals, comprising a superimposition of several sub-channel signals, often leads to an escalated PAPR when these signals converge in phase. Such a phenomenon necessitates the operation of the power amplifier in a system within a broad linear range to avert signal distortion, as illustrated in Figure 1.

The challenge of reducing the PAPR in OFDM signals has given rise to three prevalent approaches: pre-distortion, encoding, and probability methods. The pre-distortion method entails preliminary non-linear processing of signals, causing high-power signals to undergo pre-distortion. This method is characterized by its simplicity and straightforwardness, despite the introduction of in-band noise and out-band interference from the non-linear transformation [4, 5].

The encoding method deploys adjustable encoding patterns to generate multiple code groups, selecting the code group with the smallest PAPR to transmit OFDM symbols. However, the complexity and tediousness of encoding

and decoding processes mar its usability [6–9]. Furthermore, the drastic reduction in the information rate rendered by this method restricts its application to fewer sub-carriers.

Lastly, the probability method aims to reduce the peak signal occurrence probability, although it doesn't ensure PAPR reduction and may introduce some information redundancy [10–12]. Noteworthy examples of probability methods include the PTS and SLM, which modify the phase distribution of the original signals to decrease the likelihood of in-phase superposition, effectively reducing the PAPR of signals without distortion.

This study is organized as follows: Section II provides a theoretical analysis, defining PAPR, and detailing the principles of traditional PTS and μ-law Companding Transformation. Section III presents the proposed PTS-Companding method, and the subsequent sections IV and V respectively demonstrate simulation results and conclude the study.

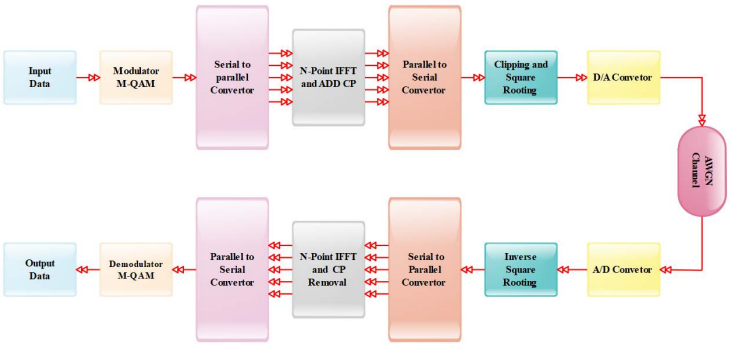

Figure 1. Fundamental block diagram of an OFDM communication system in an LTE platform

2 Theoretical Analysis

2.1 PAPR

The PAPR is defined as the ratio between the maximum power and the average power of the signal over a symbol period. The PAPR of an OFDM signal can be expressed as shown in Eq. (1):

$$PAPR(dB) = 10\log_{10}\frac{\max\left\{|a_n|^2\right\}}{F\left\{|x_n|^2\right\}} \tag{1}$$

where, a_n represents the OFDM signal post the influence of C-point Inverse Fast Fourier Transform (IFFT), as illustrated in Eq. (2):

$$a_n = \frac{1}{\sqrt{C}}\sum_{i=0}^{C-1} A_i e^{j\pi ni/C} \tag{2}$$

where, C denotes the sub-carrier index, while $A_i(0 \leq i \leq C-1)$ signifies the i^{th} complex modulated symbol in the OFDM system [13, 14]. The CCDF, illustrating the probability of the PAPR exceeding a particular threshold, is often employed to gauge the PAPR reduction capacity of a communication system [15–18].

2.2 Conventional PTS

The probability method primarily employs linear transformation, given in Eq. (3):

$$O_n = V_n A_n + W_n(1 \leq n \leq C) \tag{3}$$

where, A_n represents the original input data before IFFT in the frequency domain, and O_n symbolizes the output following the linear transformation. The probability method endeavors to identify a C-point vector V and W that can diminish the peak value occurrence probability of the transmission signals post IFFT. The PTS method initially sets vector W to zero and subsequently selects an apt vector V to reduce peak signal incidence probability. The linear transformation of PTS consists only of phase rotation, limiting the vector V's amplitude to unit amplitude [19–22].

In a PTS-OFDM system, three data partitioning methods are prevalent: adjacent partition, interleaved partition, and random division. Evidently, random division exhibits superior PAPR performance, albeit interleaved partitioning presents the least complexity. Furthermore, the PAPR in a PTS system is influenced by the number of groups V and phase factors F; an increase in either improves the PAPR, albeit at the expense of system complexity [23–28].

2.3 Companding Transformation of μ-law

The Companding Transformation employs non-uniform quantization functions, such as the μ-law and A-law companding functions, to compress high-power signals and amplify low-power signals, thus sustaining average power. This method enhances the resistance of low power signals and reduces PAPR. A critical step in this process involves the transformation of signals post-orthogonal modulation in the time domain using the Companding Transformation, a step less computationally intensive than PTS. The received signals are restored via an equivalent inverse Companding Transformation before demodulation [29–32].

A conventional Companding Transformation is the μ-law, using a non-linear transform function based on the μ-law non-uniform quantization in speech processing. It should be noted that this method introduces in-band noise and out-band interference at the receiver since the inverse Companding Transformation amplifies large signals and their noise while attenuating small signals and their noise, leading to an inferior BER [33].

3 RIA

This study explores the development of a RIA that effectively merges both the PTS and Companding Transformation to alleviate the occurrence of maximum peak signals [34]. The architecture of the proposed system is displayed in Figure 2.

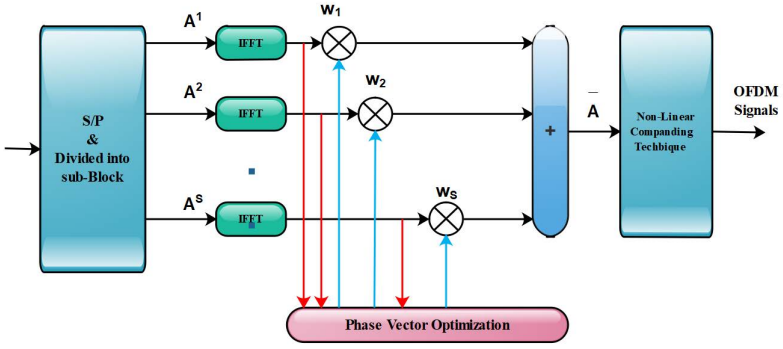

Figure 2. Functional block diagram of the proposed RIA

The original data, denoted as "*A*" is partitioned into "*S*" non-overlapping sub-blocks of length "*N*," represented as $A^s, s = 1, 2, 3, 4, \ldots\ldots S$, where s ranges from 1 to *S*. This process is outlined in Eq. (4).

$$A = \sum_{s=1}^{S} A^s \tag{4}$$

After the application of the C-point IFFT, each data block is multiplied by its corresponding phase factor, W_s. The phase factors across different data blocks are statistically independent, resulting in statistically independent phase factors within the rotation vector, as expressed in Eq. (5).

$$x = \sum_{s=1}^{S} \left(w_s \cdot \mathrm{IFFT}\left(A_s\right)\right) \tag{5}$$

The optimization of the phase vector involves selecting suitable weighted coefficients $[w_1, w_2, w_3, w_4 \ldots\ldots w_s]$ that minimize the peak values of the powers. The optimization condition for these coefficients is given in Eq. (6).

$$\{w_1, w_2, w_3, w_4 \ldots\ldots w_s\} = \underset{w_1, w_2, w_3, w_4 \ldots\ldots w_s}{\operatorname{argmin}} \left(\min_{1 \le n \le C} |A|^2 \right) \tag{6}$$

where, *argmin*(.) is the condition that allows the function to reach its lowest value [35]. Subsequently, a μ-law Companding Transformation is applied to the signal "*a*" improving the PAPR. This transformation is represented by Eq. (7).

$$a' = \frac{V_a \ln\left(1 + \mu \frac{|a|}{V}\right)}{|a| \ln(1 + \mu)} \tag{7}$$

At the receiver end, the received signal "*y*" is first transformed using the μ'-law inverse Companding Transformation, where μ' denotes the inverse companding coefficient and A' represents the normalization constant, taken as

max($|o|$) [36, 37]. The signal O', divided into sub vector signals of length C, is used to determine carrier signal side information, represented by $\{w_1, w_2, w_3, w_4 \ldots\ldots w_s\}$. A N-point FFT is then applied after dividing the O^S by the rotation factor W_S. Finally, the data blocks are added as outlined in Eq. (8).

$$O = \sum_{s=1}^{S} FFT\left(o^s / w_s\right) \tag{8}$$

This integrated approach significantly improves PAPR performance without compromising BER or transmission rate. Methods to enhance BER and maintain transmission rate are discussed in parts 1) and 2), respectively [38–40].

To counteract the poor BER performance induced by the Companding Transformation, a companding coefficient μ' at the receiver end is chosen to be less than that of the transmitter, i.e., $\mu' = I_\mu(I < 1)$. This selection reduces the noise gain of larger signals and ensures a satisfactory BER.

PTS employs an appropriate rotation vector to minimize the peak signal occurrence. The exhaustive search required to traverse all phase combinations $\{w_1, w_2, w_3, w_4 \ldots\ldots w_s\}$ is F^S, where "*S*" is the group number and "*F*" is the phase factor number. As "*S*" and "*F*" increase, the system complexity escalates [41–47].

To alleviate computational demands, a simple search is recommended when the number of phase combinations is extensive. Initially, all weighted coefficients W_S are set to 1 ($s = 1, 2, 3, 4, \ldots\ldots S$) and $b1$ is allowed to traverse every vector in the phase space. An optimal vector is selected such that the current PAPR reduction is maximized [48–54]. This selection process is repeated for the remaining weighted coefficients $w_s(s = 1, 2, 3, 4, \ldots\ldots S)$. This iterative search is typically performed three times, with negligible PAPR performance improvement beyond three iterations. While this simple search compromises PAPR reduction, it notably enhances the transmission rate when "*F*" or "*S*" is high [55–62].

4 Simulation and Analysis

The proposed RIA underwent comprehensive simulations using MATLAB, adopting the parameters delineated in Table 1. Subsequently, PAPR and BER performances were compared between the traditional PTS and μ-law Companding Transformation. An audio signal of 12KB size was employed as the input source for these simulations.

Table 1. Simulation analysis parameters

Scheme	Standard Parameters		
Convention Methods			
Companding Technique	Parameter same as proposed method		
PTS	Parameter same as proposed method		
SLM	S is the group index		5
	F is the phase factor index		4
Clipping and Filtering	Clipping cycle time		5
	Clipping ratio (CR)		5
Tone reservation (TR)	Attenuation factor		0.6
	Reserved carrier index		8
	Iteration time		11
Proposed Method			
The Reconfigurable Integrated Algorithm	C is the sub-carrier index		64
	Attenuation factor	F1	0.33
		F2	0.27
	Delay factor	D1	5
		D2	9
	Data Partitioning		Random Division
	S is the group index		5
	F is the phase factor index		3
	'I' is inverse Companding scale		4
	'γ' is the Companding coefficient		0.5
	Search simple		No

In Figure 3, a comparative analysis of PAPR performance between the proposed method and existing strategies is illustrated. Observations from Table 2 indicate reductions in both BER and elapsed time. It is evident from Figure 3 that variations in PAPR between the novel technique and established techniques such as clipping, SLM, TR, PTS, and Companding Transformation are +0.90dB, -0.80dB, -3.4dB, -0.47dB, and -7 dB, respectively, at a probability of 10^{-2}. Although clipping has superior PAPR performance, its BER is approximately six times greater. When the

novel method's factor F is adjusted to 4, the Complementary Cumulative Distribution Function (CCDF) distribution curve closely aligns with that of clipping, and the novel system's BER only increases by 0.02%. Table 2 reaffirms that the novel system can ensure a precise BER and transmission rate.

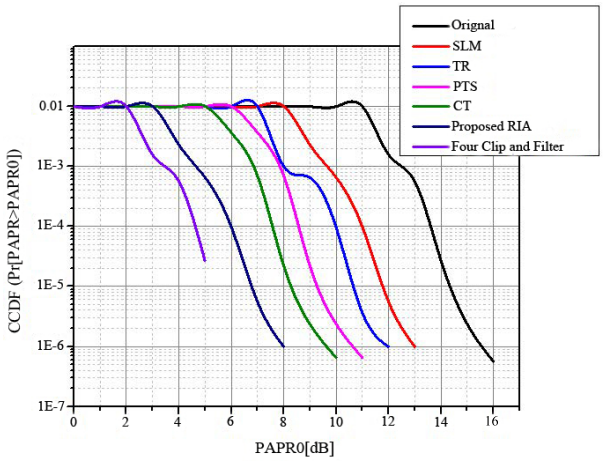

Figure 3. Performance analysis between proposed algorithm and conventional methods with respect to PARA

Table 2. Simulation analysis results

Scheme	Performance	
	BER (%)	Elapsed Time (s)
Message signal	0.08	0.62
Conventional CT	0.15	0.22
Conventional PTS	6.01	0.23
$C/\gamma = 82^*$	0.08	0.82
SLM	0.06	0.39
Clipping and Filtering	0.9	0.22
TR	0.13	16.23
Proposed RIA/ $\gamma = \mathbf{81}$	5.32	1.65
Proposed RIA/I=0.65	0.2	1.32
Proposed RIA/I=1	0.26	1.23
Proposed RIA/S=2	0.16	0.61
Proposed RIA/S=9	0.14	105.22
Proposed RIA/S=5 and simple search	0.18	2.31
Proposed RIA/S=9 and simple search	0.198	3.22

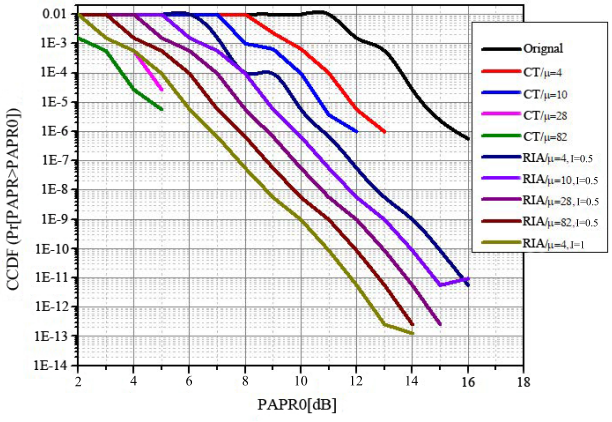

Figure 4. Performance analysis between proposed algorithm and conventional methods with respect to PARA and various μ

Figure 4 presents an analysis of PAPR performance under varying conditions of μ, specifically, when μ is 4, 10, 28, and 82. With the conventional μ-law Companding Transformation, the PAPR performance improves as μ increases, albeit at the expense of signal quality. At μ =82, the BER reaches 5.969%. Conversely, the novel system generally demonstrates a positive relationship between μ and PAPR performance, although PAPR reduction is less noticeable. At μ =82, the BER of the novel system is 5.32%, showing the signal distortion level comparable to that of the Companding Transformation. As illustrated in Figure 4, when μ is 4, and the inverse companding scale I is 0.4, 0.7, and 1, the BER is 0.13%, 0.18%, and 0.25%, respectively, even though PAPR remains relatively stable, indicating that a smaller inverse companding coefficient μ' at the receiver can improve signal quality.

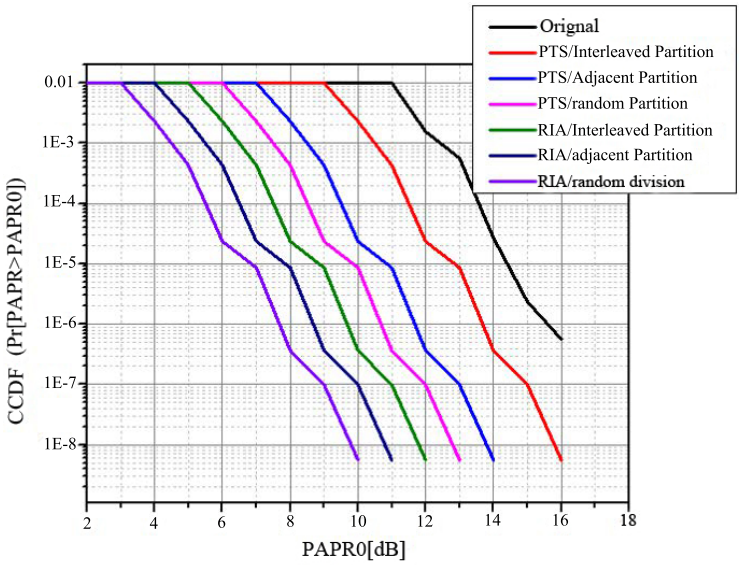

Figure 5. Performance analysis between proposed algorithm and conventional methods with respect to PARA and various groups methods

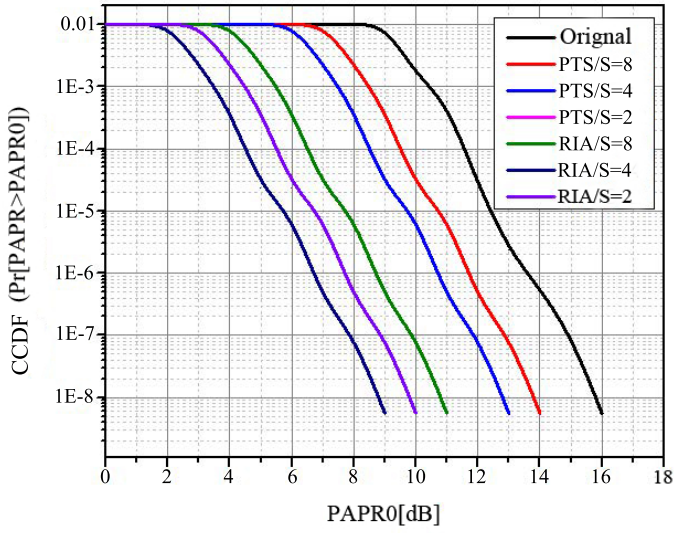

Figure 6. Performance analysis between proposed algorithm and conventional methods with respect to PARA and various groups methods

Figure 5, Figure 6 and Figure 7 showcase PAPR performance due to various factors involved in PTS, namely, data partitioning methods, group number V, and phase factor number P. The results in Figure 5 indicate that optimal PAPR performance can be achieved via random division for the novel system and PTS. According to Figure 6, the novel method can efficiently reduce PAPR of Orthogonal Frequency Division Multiplexing (OFDM) signals; the greater the group number S, the better the PAPR, but with increased system complexity.

In Figure 7, a comparison is made with a varying phase factor number P. As F increases, more options for weighted coefficients become available, improving PAPR but compromising the system's transmission rate. As S or F increases, more combinations need to be traversed to find the optimal solution, thus increasing time. However, by adopting a simplified search, PAPR reduction is somewhat weakened. The exhaustive search elapsed times are 7.19s and 104.11s for S=4/F=4 and S=4/P=8, respectively, while the elapsed times for the simplified search are 2.10s and 3.25s. This indicates a trade-off between complexity and PAPR performance.

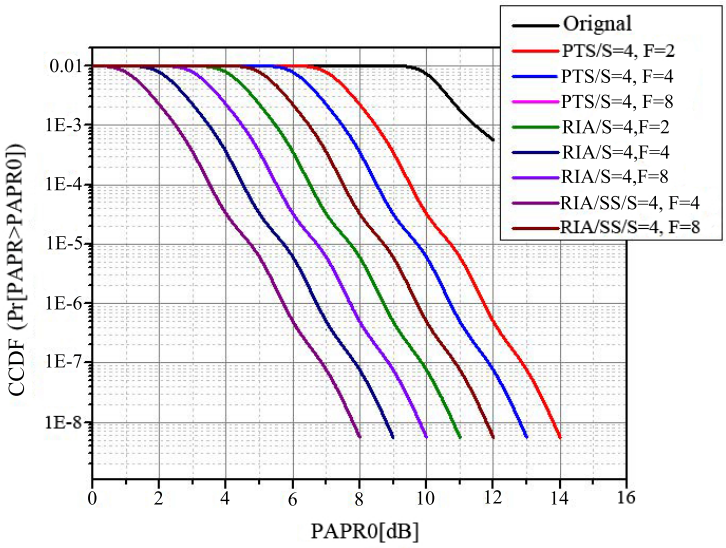

Figure 7. Performance analysis between proposed algorithm and conventional methods with respect to PARA and various phase methods

To provide a more comprehensive understanding of the proposed technique, future work could include a detailed breakdown of the PTS method, including further elucidation on the effect of group number V and phase factor number P on PAPR performance. This could also be supplemented by an extensive discussion on why the simple search strategy affects PAPR reduction and how this trade-off impacts real-world applications of the system.

5 Conclusion

This study prioritized the mitigation of PAPR in an OFDM system utilizing the proposed RIA. Analyses indicate a lower CCID of the proposed RIA compared to the traditional PTS method, given S=8,4,2. Additionally, with respect to μ=4,10,28,82, the RIA has demonstrated superior performance over the conventional CT technique in terms of CCID.

Considering the methods of interleaved partition, adjacent partition, and random partition for determining the CCDF between the proposed RIA and conventional PTS, simulation analyses have demonstrated the superior performance of RIA. The RIA algorithm has effectively integrated the PTS and CT to decrease PAPR to 0.55dB and 0.656dB compared to the respective PTS and CT algorithms. A reduction of signal distribution by 0.02% relative to conventional methods was observed.

Elapsed times for the exhaustive PAPR search were determined as 7.65s and 104.12s for S=4/F=4 and S=4/F=8, respectively. For the simplified search, elapsed times were recorded as 2.10s and 3.25s.

Looking ahead, the proposed algorithm may offer significant enhancements to the BER and transmission rates of future wireless communication technologies such as 5G and 6G. As a rising number of urban environments transition to smart city infrastructures, an increasing volume of data communication will occur via IoT devices. These innovations necessitate highly accurate and rapid communication processes. The proposed methods, albeit necessitating more parallel operations, demonstrate potential compatibility with 6G communication processes.

Limitations were identified in operating the OFDM communication system within 6G technology, where parallel operations can generate jitters and hazards, leading to signal attenuation. These effects could compromise the accuracy of long-distance communication and result in a loss of original information.

Future research may benefit from a comprehensive examination of how the proposed RIA algorithm performs under different real-world conditions, especially within the context of smart city infrastructures. Furthermore, studies could delve into mitigating the limitations identified in this research, particularly those related to long-distance communication accuracy and the handling of information loss. These advancements could support the

adaptation of the proposed RIA algorithm for future wireless communication technologies, ensuring accurate and fast communication for increasingly data-driven environments.

Data Availability

The data used to support the findings of this study are available from the corresponding author upon request.

Conflicts of Interest

The authors declare that they have no conflicts of interest.

References

[1] M. M. Rana and L. Li, "Kalman filter based microgrid state estimation using the Internet of Things communication network," in *2015 12th International Conference on Information Technology - New Generations*, Las Vegas, NV, USA, 2015, pp. 501–505. https://doi.org/10.1109/ITNG.2015.86

[2] M. Sun and Z. Sahinoglu, "Extended Kalman filter based grid synchronization in the presence of voltage unbalance for smart grid," in *ISGT 2011*, Anaheim, CA, USA, 2011, pp. 1–4. https://doi.org/10.1109/ISGT.2011.5759147

[3] P. Satish, M. Srikantaswamy, and N. K. Ramaswamy, "A comprehensive review of blind deconvolution techniques for image deblurring," *Trait. Signal*, vol. 37, no. 3, pp. 527–539, 2020. https://doi.org/10.18280/ts.370321

[4] M. Khalaf, A. Youssef, and E. El-Saadany, "Detection of false data injection in automatic generation control systems using Kalman filter," in *2017 IEEE Electrical Power and Energy Conference (EPEC)*, Saskatoon, SK, Canada, 2017, pp. 1–6. https://doi.org/10.1109/EPEC.2017.8286194

[5] H. N. Mahendra, S. Mallikarjunaswamy, V. Rekha, V. Puspalatha, and N. Sharmila, "Performance analysis of different classifier for remote sensing application," *Inter. J. Engi. & Advanced Tech.*, vol. 9, no. 1, pp. 7153–7158, 2019. https://doi.org/10.35940/ijeat.A1879.109119

[6] S. Thazeen, S. Mallikarjunaswamy, G. K. Siddesh, and N. Sharmila, "Conventional and subspace algorithms for mobile source detection and radiation formation," *Trait. Signal*, vol. 38, no. 1, pp. 135–145, 2021. https://doi.org/10.18280/ts.380114

[7] H. N. Mahendra, S. Mallikarjunaswamy, G. K. Siddesh, M. Komala, and N. Sharmila, "Evolution of real-time onboard processing and classification of remotely sensed data," *Indian J. Sci. Tech.*, vol. 13, no. 20, pp. 2010–2020, 2020. https://doi.org/10.17485/IJST/v13i20.459

[8] M. M. Rana and L. Li, "Distributed generation monitoring of smart grid using accuracy dependent Kalman filter with communication systems," in *2015 12th International Conference on Information Technology - New Generations*, Las Vegas, NV, USA, 2015, pp. 496–500. https://doi.org/10.1109/ITNG.2015.154

[9] Y. Wang, Z. Zhang, J. Ma, and Q. Jin, "Kfrnn: An effective false data injection attack detection in smart grid based on Kalman filter and recurrent neural network," *IEEE Internet Things J.*, vol. 9, no. 9, pp. 6893–6904, 2021. https://doi.org/10.1109/JIOT.2021.3113900

[10] S. Chaitra, "A comprehensive review of parallel concatenation of ldpc code techniques," *Indian J. Sci. Tech.*, vol. 14, no. 5, pp. 432–444, 2021. https://doi.org/10.17485/IJST/v13i20.459

[11] Y. Liu and L. Cheng, "Relentless false data injection attacks against Kalman filter based detection in smart grid," *IEEE Trans. Control Netw. Syst.*, vol. 9, no. 3, pp. 1238–1250, 2022. https://doi.org/10.1109/TCNS.2022.3141026

[12] J. Sawodny, O. Riedel, and T. Namerikawa, "Detection of attacks in smart grids via extended Kalman filter and correlation analysis," in *2020 59th Annual Conference of the Society of Instrument and Control Engineers of Japan (SICE)*, Chiang Mai, Thailand, 2020, pp. 663–669. https://doi.org/10.23919/SICE48898.2020.9240229

[13] M. L. Umashankar, T. N. Anitha, and S. Mallikarjunaswamy, "An efficient hybrid model for cluster head selection to optimize wireless sensor network using simulated annealing algorithm," *Indian J. Sci. Tech.*, vol. 14, no. 3, pp. 270–288, 2021. https://doi.org/10.17485/IJST/v14i3.2318

[14] R. Shivaji, "Design and implementation of reconfigurable DCT based adaptive PST techniques in OFDM communication system using interleaver encoder," *Indian J. Sci. Tech.*, vol. 13, no. 29, pp. 3008–3020, 2020. https://doi.org/10.17485/IJST/v13i29.976

[15] M. L. Umashankar, M. V. Ramakrishna, and S. Mallikarjunaswamy, "Design of high speed reconfigurable deployment intelligent genetic algorithm in maximum coverage wireless sensor network," in *2019 International Conference on Data Science and Communication (IconDSC)*, Bangalore, India, 2019, pp. 1–6. https://doi.org/10.1109/IconDSC.2019.8816930

[16] M. M. Rana, R. Bo, and B. J. Choi, "Residual saturation based Kalman filter for smart grid state estimation under cyber attacks," in *2019 IEEE 9th Annual International Conference on CYBER Technology in Automation,*

Control, and Intelligent Systems (CYBER), Suzhou, China, 2019, pp. 1459–1463. https://doi.org/10.1109/CYBER46603.2019.9066737

[17] S. Mallikarjunaswamy, K. R. Nataraj, and K. R. Rekha, *Design of high-speed reconfigurable coprocessor for next-generation communication platform*. Springer India, 2014, pp. 57–67. https://doi.org/10.1007/978-81-322-1157-0_7

[18] S. Mallikarjunaswamy, K. R. Nataraj, P. Balachandra, and N. Sharmila, "Design of high speed reconfigurable coprocessor for interleaver and de-interleaver operations," *J. Impact Factor*, vol. 6, no. 1, pp. 30–38, 2015.

[19] Y. Zhang, H. Wang, and H. Wang, "Integrated navigation positioning algorithm based on improved Kalman filter," in *2017 International Conference on Smart Grid and Electrical Automation (ICSGEA)*, Changsha, China, 2017, pp. 255–259. https://doi.org/10.1109/ICSGEA.2017.55

[20] A. C. Savitha, M. N. Jayaram, and S. M. Swamy, "Development of energy efficient and secure routing protocol for m2m communication," *Int. J. Performability Eng.*, vol. 18, no. 6, pp. 426–433, 2022. https://doi.org/10.23940/ijpe.22.06.p5.426-433

[21] D. Y. Venkatesh, K. Mallikarjunaiah, and M. Srikantaswamy, "A comprehensive review of low density parity check encoder techniques," *Ing. Syst. Inf.*, vol. 27, no. 1, pp. 11–20, 2022. https://doi.org/10.18280/isi.270102

[22] S. Pooja, S. Mallikarjunaswamy, and N. Sharmila, "Adaptive sparsity through hybrid regularization for effective image deblurring," *Indian J. Sci. Tech.*, vol. 14, no. 24, pp. 2051–2068, 2021. https://doi.org/10.17485/IJST/v14i24.604

[23] Y. Jiang and Q. Hui, "Kalman filter with diffusion strategies for detecting power grid false data injection attacks," in *2017 IEEE International Conference on Electro Information Technology (EIT)*, Lincoln, NE, USA, 2017, pp. 254–259. https://doi.org/10.1109/EIT.2017.8053365

[24] F. Akbarian, A. Ramezani, M. T. Hamidi-Beheshti, and V. Haghighat, "Intrusion detection on critical smart grid infrastructure," in *2018 Smart Grid Conference (SGC)*, 2018, pp. 1–6. https://doi.org/10.1109/SGC.2018.8777815

[25] R. Shivaji, K. R. Nataraj, S. Mallikarjunaswamy, and K. R. Rekha, *Implementation of an effective hybrid partial transmit sequence model for peak to average power ratio in MIMO OFDM System*, ser. Lecture Notes in Electrical Engineering. Springer, 2020, vol. 783. https://doi.org/10.1007/978-981-16-3690-5_129

[26] S. Thazeen and S. Mallikarjunaswamy, "The effectiveness of 6t beamformer algorithm in smart antenna systems for convergence analysis," *IIUM Eng. J.*, vol. 24, no. 2, pp. 100–116, 2023. https://doi.org/10.31436/iiumej.v24i2.2730

[27] N. Zhou, D. Meng, Z. Huang, and G. Welch, "Dynamic state estimation of a synchronous machine using PMU data: A comparative study," *IEEE Trans. Smart Grid*, vol. 6, no. 1, pp. 450–460, 2015. https://doi.org/10.1109/TSG.2014.2345698

[28] H. N. Mahendra, S. Mallikarjunaswamy, C. B. Nooli, M. Hrishikesh, N. Kruthik, and H. M. Vakkalanka, "Cloud based centralized smart cart and contactless billing system," in *2022 7th International Conference on Communication and Electronics Systems (ICCES)*, Coimbatore, India, 2022, pp. 820–826. https://doi.org/10.1109/ICCES54183.2022.9835856

[29] T. N. Manjunath, M. Komala, and K. S. Manu, "An efficient hybrid reconfigurable wind gas turbine power management system using MPPT algorithm," *Int. J. Power Electro. Drive Syst.*, vol. 12, no. 4, pp. 2501–2510, 2021. https://doi.org/10.11591/ijpeds.v12.i4.pp2501-2510

[30] J. Sawodny, O. Riedel, and T. Namerikawa, "Detection of attacks in smart grids via extended Kalman filter and correlation analysis," in *2020 59th Annual Conference of the Society of Instrument and Control Engineers of Japan (SICE)*, Chiang Mai, Thailand, 2020, pp. 663–669. https://doi.org/10.23919/SICE48898.2020.9240229

[31] J. Zhao and L. Mili, "A decentralized h-infinity unscented Kalman filter for dynamic state estimation against uncertainties," *IEEE Trans. Smart Grid*, vol. 10, no. 5, pp. 4870–4880, 2020. https://doi.org/10.1109/TSG.2018.2870327

[32] S. Pooja, S. Mallikarjunaswamy, and N. Sharmila, "Hybrid regularization algorithm for efficient image deblurring," *Int. J. Eng. Adv. Technol.*, vol. 10, no. 6, pp. 141–147, 2021. https://doi.org/10.35940/ijeat.F2998.0810621

[33] M. M. Pandith, N. K. Ramaswamy, M. Srikantaswamy, and R. K. Ramaswamy, "A comprehensive review of geographic routing protocols in wireless sensor network," *Inform. Dyn. Appl.*, vol. 1, no. 1, pp. 14–25, 2022. https://doi.org/10.56578/ida010103

[34] H. N. Mahendra and S. Mallikarjunaswamy, "An efficient classification of hyperspectral remotely sensed data using support vector machine," *Int. J. Electro. Telecom.*, vol. 68, no. 3, pp. 609–617, 2022. https://doi.org/10.24425/ijet.2022.141280

[35] M. M. Rana, "Extended Kalman filter based distributed state estimation algorithm for cyber physical systems," in *2018 3rd International Conference on Inventive Computation Technologies (ICICT)*, Coimbatore, India,

2018, pp. 653–655. https://doi.org/10.1109/ICICT43934.2018.9034255

[36] K. Manandhar, X. Cao, F. Hu, and Y. Liu, "Combating false data injection attacks in smart grid using Kalman filter," in *2014 International Conference on Computing, Networking and Communications (ICNC)*, Honolulu, HI, USA, 2014, pp. 16–20. https://doi.org/10.1109/ICCNC.2014.6785297

[37] M. L. Umashankar, S. Mallikarjunaswamy, and M. V. Ramakrishna, "Design of high speed reconfigurable distributed life time efficient routing algorithm in wireless sensor network," *J. Comput. Theor. Nanosci.*, vol. 17, no. 9-10, pp. 3860–3866, 2020. https://doi.org/10.1166/jctn.2020.8975

[38] S. P. Talebi, S. Kanna, and D. P. Mandic, "A distributed quaternion Kalman filter with applications to smart grid and target tracking," *IEEE Trans. Signal Inform. Process. Netw.*, vol. 2, no. 4, pp. 477–488, 2016. https://doi.org/10.1109/TSIPN.2016.2618321

[39] S. Rathod and N. K. Ramaswamy, "An efficient reconfigurable peak cancellation model for peak to average power ratio reduction in orthogonal frequency division multiplexing communication system," *Int. J. Electr. Comput. Eng.*, vol. 12, no. 6, pp. 6239–6247, 2022. https://doi.org/10.11591/ijece.v12i6

[40] S. Shebin and S. Mallikarjunaswamy, "A software tool that provides relevant information for diabetic patients to help prevent diabetic foot," *IOSR J. Comput. Eng.*, vol. 16, no. 2, pp. 69–73, 2014. https://doi.org/10.9790/0661-16296973

[41] M. L. Umashankar, S. Mallikarjunaswamy, N. Sharmila, D. M. Kumar, and K. R. Nataraj, "A survey on iot protocol in real-time applications and its architectures," in *ICDSMLA 2021. Lecture Notes in Electrical Engineering*, vol. 947. Springer, Singapore, 2023. https://doi.org/10.1007/978-981-19-5936-3_12

[42] S. Mallikarjunaswamy, N. Sharmila, G. K. Siddesh, K. R. Nataraj, and M. Komala, *A novel architecture for cluster based false data injection attack detection and location identification in smart grid*. Springer, Singapore, 2022. https://doi.org/10.1007/978-981-16-3497-0_48

[43] S. Mallikarjunaswamy, N. Sharmila, D. Maheshkumar, M. Komala, and H. N. Mahendra, "Implementation of an effective hybrid model for islanded microgrid energy management," *Indian J. Sci. Tech.*, vol. 13, no. 27, pp. 2733–2746, 2020. https://doi.org/10.17485/IJST/v13i27.982

[44] T. A. Madhu, M. Komala, V. Rekha, S. Mallikarjunaswamy, N. Sharmila, and S. Pooja, "Design of fuzzy logic controlled hybrid model for the control of voltage and frequency in microgrid," *Indian J. Sci. Tech.*, vol. 13, no. 35, pp. 3612–3629, 2020. https://doi.org/10.17485/IJST/v13i35.1510

[45] V. P. Bhuvana, M. Huemer, and A. Tonello, "Battery internal state estimation using a mixed Kalman cubature filter," in *2015 IEEE International Conference on Smart Grid Communications (SmartGridComm)*, Miami, FL, USA, 2015, pp. 521–526. https://doi.org/10.1109/SmartGridComm.2015.7436353

[46] R. Mohammadrezaee, J. Ghaisari, G. Yousefi, and M. Kamali, "Dynamic state estimation of smart distribution grids using compressed measurements," *IEEE Transactions on Smart Grid*, vol. 12, no. 5, pp. 4535–4542, 2021. https://doi.org/10.1109/TSG.2021.3071514

[47] B. Özsoy and M. Göl, "A hybrid state estimation strategy with optimal use of pseudo-measurements," in *2018 IEEE PES Innovative Smart Grid Technologies Conference Europe (ISGT-Europe)*, Sarajevo, Bosnia and Herzegovina, 2018, pp. 1–6. https://doi.org/10.1109/ISGTEurope.2018.8571513

[48] M. M. Rana, M. K. R. Khan, and A. Abdelhadi, "IoT architecture for cyber-physical system state estimation using unscented Kalman filter," in *2020 Second International Conference on Inventive Research in Computing Applications (ICIRCA)*, Coimbatore, India, 2020, pp. 910–913. https://doi.org/10.1109/ICIRCA48905.2020.9183350

[49] P. Nayak and B. N. Sahu, "A robust extended Kalman filter for the estimation of time varying power system harmonics in noise," in *2015 IEEE Power, Communication and Information Technology Conference (PCITC)*, Bhubaneswar, India, 2015, pp. 635–640. https://doi.org/10.1109/PCITC.2015.7438074

[50] S. Thazeen, S. Mallikarjunaswamy, M. N. Saqhib, and S. N., "DOA method with reduced bias and side lobe suppression," in *2022 International Conference on Communication, Computing and Internet of Things (IC3IoT)*, Chennai, India, 2022, pp. 1–6. https://doi.org/10.1109/IC3IOT53935.2022.9767996

[51] S. Shebin and S. Mallikarjunaswamy, "A review on clinical decision support system and its scope in medical field," *Inter. J. Engi. Res. & Tech.*, pp. 417–420, 2018. https://doi.org/10.17577/IJERTV7IS020103

[52] S. Pooja, M. Mallikarjunaswamy, and S. Sharmila, "Image region driven prior selection for image deblurring," *Multimed. Tools Appl.*, 2023. https://doi.org/10.1007/s11042-023-14335-y

[53] H. N. Mahendra, S. Mallikarjunaswamy, D. M. Kumar, S. Kumari, S. Kashyap, S. Fulwani, and A. Chatterjee, "Assessment and prediction of air quality level using arima model: A case study of Surat City, Gujarat State, India," *Nat. Environ. Pollut. Technol.*, vol. 22, no. 1, pp. 199–210, 2023. https://doi.org/10.46488/NEPT.2023.v22i01.018

[54] P. M. B. Muddumadappa, S. D. K. Anjanappa, and M. Srikantaswamy, "An efficient reconfigurable cryptographic model for dynamic and secure unstructured data sharing in multi-cloud storage server," *J.*

Intell Syst. Control, vol. 1, no. 1, pp. 68–78, 2022. https://doi.org/10.56578/jisc010107

[55] S. Thazeen, S. Mallikarjunaswamy, and M. N. Saqhib, "Septennial adaptive beamforming algorithm," in *2022 International Conference on Smart Information Systems and Technologies (SIST)*, Nur-Sultan, Kazakhstan, 2022, pp. 1–4. https://doi.org/10.56578/jisc010107

[56] R. S., K. R. Nataraj, S. Rekha, and Mallikarjunaswamy, "Comprehensive review of optimal utilization of clock and power resources in multi bit flip flop techniques," *Indian J. Sci. Tech.*, vol. 14, no. 44, pp. 3270–3279, 2021. https://doi.org/10.17485/IJST/v14i44.1790

[57] H. N. Mahendra, S. Mallikarjunaswamy, and S. R. Subramoniam, "An assessment of vegetation cover of Mysuru City, Karnataka State, India, using deep convolutional neural networks," *Environ. Monit. Assess.*, vol. 195, pp. 1–11, 2023. http://doi.org/10.1007/s10661-023-11140-w

[58] M. M. Pandith, N. K. Ramaswamy, M. Srikantaswamy, and R. K. Ramaswamy, "A comprehensive review of geographic routing protocols in wireless sensor network," *Inf. Dyn. Appl.*, vol. 1, no. 1, pp. 14–25, 2022. https://doi.org/10.56578/ida010103

[59] H. N. Mahendra and S. Mallikarjunaswamy, "An assessment of built-up cover using geospatial techniques – a case study on Mysuru District, Karnataka State, India," *Int. J. Environ. Tech. Manag.*, vol. 26, no. 5, pp. 173–188, 2023. https://doi.org/10.1504/IJETM.2023.130787

[60] S. Mallikarjunaswamy, N. M. Basavaraju, N. Sharmila, H. N. Mahendra, S. Pooja, and B. L. Deepak, "An efficient big data gathering in wireless sensor network using reconfigurable node distribution algorithm," in *2022 Fourth International Conference on Cognitive Computing and Information Processing (CCIP)*, Bengaluru, India, 2022, pp. 1–6. https://doi.org/10.1109/CCIP57447.2022.10058620

[61] H. N. Mahendra, S. Mallikarjunaswamy, N. M. Basavaraju, P. M. Poojary, P. S. Gowda, M. Mukunda, B. Navya, and V. Pushpalatha, "Deep learning models for inventory of agriculture crops and yield production using satellite images," in *2022 IEEE 2nd Mysore Sub Section International Conference (MysuruCon)*, Mysuru, India, 2022, pp. 1–7. https://doi.org/10.1109/MysuruCon55714.2022.9972523

[62] G. S. Pavithra, S. Pooja, V. Rekha, H. N. Mahendra, N. Sharmila, and S. Mallikarjunaswamy, *Comprehensive Analysis on Vehicle-to-Vehicle Communication Using Intelligent Transportation System*. Springer, 2023, vol. 1449. https://doi.org/10.1007/978-981-99-3608-3_62